# Interpolyelectrolyte Complexes of Dynamic Multicompartment Micelles

**Felix Schacher,[†,*] Eva Betthausen,[†] Andreas Walther,[†,‡] Holger Schmalz,[†] Dmitry V. Pergushov,[§] and Axel H. E. Müller[†,*]**

[†]Makromolekulare Chemie II and Bayreuther Zentrum für Kolloide und Grenzflächen, Universität Bayreuth, Universitätsstrasse 30, D-95440 Bayreuth, Germany, [‡]Department of Applied Physics, Helsinki University of Technology, FIN-02015 TKK, Helsinki, Finland, and [§]Department of Polymer Science, School of Chemistry, Moscow State University, Vorob'evy Gory, 119991 Moscow, Russia

**ABSTRACT** Dynamic core—shell—shell—corona micelles are formed between two oppositely charged block copolymer systems. Preformed polybutadiene-*block*-poly(*N*-methyl-2-vinylpyridinium)-*block*-poly(methacrylic acid) (PB-P2VPq-PMAA) block terpolymer micelles with a soft polybutadiene core, an interpolyelectrolyte complex (IPEC) shell made out of poly(*N*-methyl-2-vinylpyridinium) and poly(methacrylic acid), and a negatively charged PMAA corona were mixed in different ratios at high pH with positively charged poly(*N*-methyl-2-vinylpyridinium)-*block*-poly(ethylene oxide) (P2VPq-PEO) diblock copolymers. Under these conditions, mixing results in the formation of a second IPEC shell onto the PB-P2VPq-PMAA precursor micelles, surrounded by a PEO corona. The resulting multicompartmented IPECs exhibit dynamic behavior, highlighted by a structural relaxation within a period of 10 days, investigated by dynamic light scattering (DLS), cryogenic transmission electron microscopy (cryo-TEM), and scanning force microscopy (SFM). After a short mixing time of 1 h, the IPECs exhibit a star-shaped structure, whereas after 10 days, spherical core—shell—shell—corona objects could be observed. To further increase complexity and versatility of the presented systems, the *in situ* formation of gold nanoparticles (Au NPs) in both the precursor micelles and the equilibrated IPEC was tested. For the PB-P2VPq-PMAA micelles, NP formation resulted in narrowly distributed Au NPs located within the PMAA shell, whereas for the core—shell—shell—corona IPEC, the Au NPs were confined within the IPEC shell and shielded from the outside through the PEO corona.

**KEYWORDS:** dynamic multicompartment micelles · interpolyelectrolyte complexes · hybrid materials · gold nanoparticles

Bottom-up processes are one of the key strategies for the preparation of materials matching the demands of today's and future nanotechnology.[1,2] Such requirements are, for example, defect-free spatial ordering over several micrometers, control over interfacial energies, or the positioning of different functional groups within close proximity. During the last decades, co- or self-assembly processes have proven to be the method of choice, providing tailored materials through the careful adjustment of supramolecular and interfacial forces and interactions. Often, block copolymers with suitable functional moieties in different compartments are taken as unimolecular building blocks for the formation of compartmentalized structures in the bulk,[3−5] in thin films,[6,7] or in solution.[8−10] In all of these cases, the driving force for structural evolution originates from the mutual incompatibility of the unlike segments. Another facile and straightforward method to induce co-assembly of block copolymers is the formation of interpolyelectrolyte complexes (IPECs) through electrostatic interactions between two oppositely charged segments,[11] either inter-[12] or intramolecular.[13] Furthermore, these interpolyelectrolyte complexes are capable of undergoing dynamic polyion exchange reactions, rendering smart colloidal objects responsive to changes in pH or salinity.[14−18]

The formation of so-called hybrid or composite materials is another way to generate structures with manifold functionalities. The most common examples are organic—inorganic hybrid materials where metal or semiconductor nanoparticles are incorporated into a polymeric matrix material.[19−22] The idea behind it is the combination of both the unique properties of metal nanoparticles regarding catalysis,[23] chemical sensing,[24] or data storage together with the cohesion, the processability, and the flexibility of polymer chains. Moreover, if carried out in solution, nanoparticles generated in this way are significantly stabilized through the coordination to the polymer chains, preventing further aggregation taking place and facilitating a narrow particle size distribution,[25] which is directly related to the materials' properties.[26,27] A prominent example are hybrid materials of block copolymers and gold nanoparticles, both in the bulk[28] and in solution.[29] Gold nanoparticles are of particular interest due to their electronic and optic properties but also due to their biocompatibility.[25]

*Address correspondence to axel.mueller@uni-bayreuth.de, felix.schacher@uni-bayreuth.de.

Received for review February 3, 2009 and accepted July 27, 2009.

**Published online August 5, 2009.** 10.1021/nn900110s CCC: $40.75

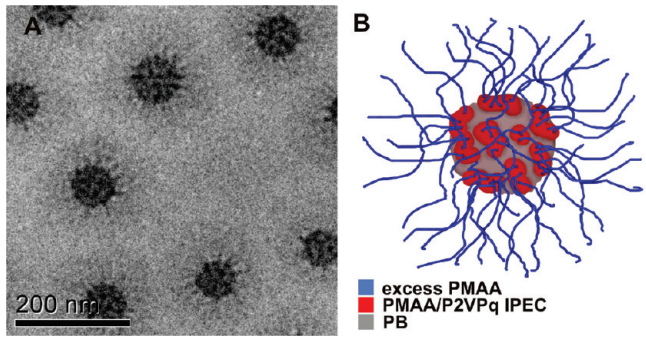


**Figure 1. Cryo-TEM of $B_{800}Vq_{190}MAA_{550}$ micelles at pH 10 (A); proposed multicompartment architecture of the micelles (B).[13]**

Within this work, we present a combination of all three previously mentioned approaches for the generation of novel complex materials: first, the self-assembly of an amphiphilic ABC block terpolymer in a selective solvent and the generation of dynamic complex multicompartment micelles. Second, the electrostatically driven co-assembly at pH 10 between negatively charged polybutadiene-*block*-poly(*N*-methyl-2-vinylpyridinium)-*block*-poly(methacrylic acid) (PB-P2VPq-PMAA, the degree of polymerization for PMAA has to be significantly higher than that for P2 VPq) block terpolymer micelles and positively charged poly(*N*-methyl-2-vinylpyridinium)-*block*-poly(ethylene oxide) (P2 VPq-PEO) diblock copolymers is investigated. Finally, the synthesis and encapsulation of narrowly dispersed gold nanoparticles within the intermediate shell of these IPECs is presented.

Both polymers were synthesized *via* living sequential anionic polymerization. Upon mixing at certain *Z* ratios (*Z* (±) being the overall ratio of positive to negative charges), core−shell−shell−corona IPECs are formed with a soft PB core, two adjacent IPEC shells consisting of PMAA and P2VPq, and a PEO corona. We show that these complexes first exhibit a star-like appearance which changes to a spherical shape during 10 days due to the dynamic nature of such IPECs. For $Z(\pm) < 1$, uncomplexed PMAA is still present in the intermediate shell formed by both PMAA and P2VPq, providing a suitable environment for the *in situ* formation of gold nanoparticles. After preparation, these nanoparticles are protected by the outer PEO shell. The aggregates were analyzed with light scattering, scanning force (SFM), and transmission electron microscopy (TEM, cryo-TEM).

## RESULTS AND DISCUSSION

**Dynamic Multicompartment Micelles from $B_{800}Vq_{190}MAA_{550}$.** Recently, we reported on the unique micellization behavior of polybutadiene-*block*-poly(*N*-methyl-2-vinylpyridinium)-*block*-poly(methacrylic acid) $B_{800}Vq_{190}MAA_{550}$ ($M_n$ = 110 kg/mol, PDI = 1.02) block terpolymers in aqueous systems. The subscripts denote the number-average degrees of polymerization of the corresponding block. Dynamic multicompartment micelles which showed response to changes in salinity or pH were formed and exhaustively characterized.[13] A cryo-TEM micrograph of such micelles at pH 10 and the proposed solution structure are shown in Figure 1. The micelles consist of a soft polybutadiene core, a patchy intramicellar interpolyelectrolyte complex shell formed by P2VPq and parts of the PMAA, and a negatively charged and, thus, stretched corona of excess PMAA (DP (PMAA) > DP (P2VPq)).

**Interpolyelectrolyte Complex Formation between $B_{800}Vq_{190}MAA_{550}$ and $Vq_{94}EO_{1245}$.** For the IPEC formation, these aggregates were mixed with quaternized poly(1-methyl-2-vinylpyridinium)-*block*-poly(ethylene oxide) $Vq_{94}EO_{1245}$ diblock copolymers in a ratio so that the overall ratio of positive to negative charges $Z = 1$ (taking into account the estimated quaternization efficiency of 80% for the P2VPq block). The degrees of polymerization are 94 (Vq) and 1250 (EO). The mixing process as well as the proposed structure of the resulting IPECs is shown in Figure 2. As described earlier,[13] we assume a remaining DP of 360 of the negatively charged PMAA for the multicompartment micellar precursor after the intramicellar IPEC formation. More precisely, for one molecule $B_{800}Vq_{190}MAA_{550}$, approximately 3.8 molecules $Vq_{94}EO_{1245}$ are added.

By mixing with positively charged $Vq_{94}EO_{1245}$ diblock copolymers in solution at pH 10, further IPEC formation takes place, providing a new shell around the PB core, as depicted in the right part of Figure 2. Although, for clarity reasons, the right part in Figure 2 displays two different IPEC shells (the red one being the former patchy shell of the precursor particles and the orange shell the newly formed IPEC) surrounding the PB core, it is rather unlikely that both can be distinguished, as they consist of the same two charged polymer segments. After IPEC formation, the whole core−shell−shell micelle is further surrounded by a PEO corona, depicted in green in Figure 2. Dynamic light scattering (DLS) was performed to compare both solutions

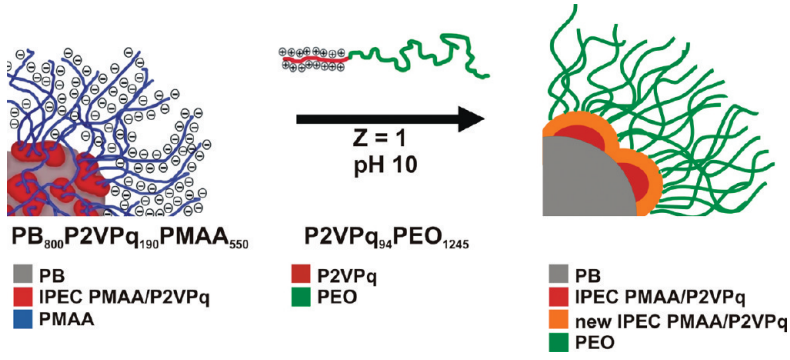


**Figure 2. Formation of IPECs between negatively charged $B_{800}V_{190}MAA_{550}$ block terpolymer micelles and positively charged $Vq_{94}EO_{1250}$ diblock copolymers at $Z(\pm) = 1$; please note that the precursor micelles on the left are shown according to an "on-top" view, whereas the IPEC on the right is shown as a cross section.**

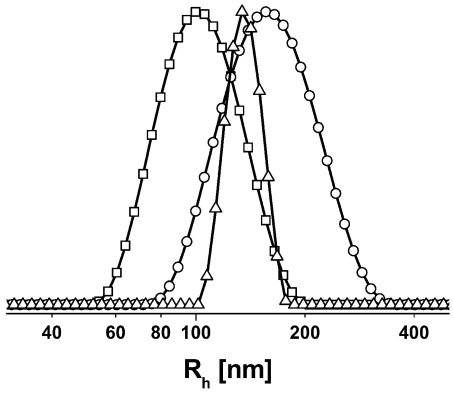


**Figure 3. DLS CONTIN plots for the $B_{800}Vq_{190}MAA_{550}$ block terpolymer precursor micelles ($<R_h>_z$ = 99 nm, PDI = 1.18, □), the IPECs at $Z(\pm) = 1$ after 1 h ($<R_h>_z$ = 155 nm, PDI = 1.19, ○) and 10 days mixing time ($<R_h>_z$ = 133 nm, PDI = 1.08, △).**

(Figure 3). The "precursor" micelles have a hydrodynamic radius $<R_h>_z$ = 99 nm (PDI = 1.18). After 1 h of mixing at $Z = 1$, the size of the aggregates increased significantly, resulting in $<R_h>_z$ = 155 nm (PDI = 1.19). Moreover, if the same experiment is performed again after 10 days, the radius decreased to 133 nm (PDI = 1.08). No significant decrease in size was observed after these 10 days. Furthermore, the distribution of the hydrodynamic radii significantly narrows after 10 days, indicating a certain equilibration of the system.

One possible explanation is that the formed IPECs are capable of undergoing polyion exchange reactions in aqueous solution and that this is the effect of some structural rearrangement of the formed polymeric micelles.[11,17] To evaluate this, cryo-TEM of a sample was performed 1 h after mixing (Figure 4A,B).

Figure 4A displays star-like micellar aggregates with a radius of around 125 nm. The PB core has a radius of 30−35 nm and is surrounded first by a very thin dark ring ($d \sim 10$ nm) and then by a 10−20 nm thick lighter gray shell ending up in several (typically 12−16) stretched arms. In Figure 4B, at a first glance, the structure appears similar, but the thin dark ring around the PB core has almost vanished and the surrounding gray shell is thicker and more continuous. Also the arms appear shorter if compared to Figure 4A. In our opinion, panels A and B in Figure 4 represent different states of a dynamic system on its way to equilibrium. A possible illustration for the formation of this intermediate structure is shown in Figure 5. Such structural rearrangements after the initial formation of an IPEC have been reported for the IPEC formation between polyisobutylene-*block*-poly(methacrylic acid) micelles with positively charged poly(*N*-ethyl-4-vinylpyridinium).[15]

In the beginning, the corona chains of $B_{800}Vq_{190}MAA_{550}$ micelles at pH 10 are charged and, hence, stretched. The same accounts for the positively charged part of $Vq_{94}EO_{1245}$. Upon mixing, first IPEC formation takes place between two stretched, oppositely charged polymer chains. Afterward, upon charge neutralization and, thus, less repulsion between the chain segments, the formed IPECs start to fuse, form a continuous shell around the PB core, and overlap with the already existing "patchy" shell of the precursor micelles. The star-like appearance of the aggregates in Figure 4A,B could be explained in this way. If the aggregation number determined for the precursor micelles ($N_{agg}$ = 243)[13] is taken into account, each of these "ray-like" protrusions should consist of 15−20 PMAA chains and the respective 3.8-fold number of oppositely charged P2VPq chains. Furthermore, the thin dark ring around the PB core in Figure 4A seems to represent the former, noncontinuous shell of the $B_{800}Vq_{190}MAA_{550}$ multicompartment micelles. Figure 4B depicts a system already somewhat closer to equilibrium, visible by the thicker and more developed IPEC shell around the PB core and the shorter arms. In addition, the dark ring has almost vanished, indicating the formation of a continuous interface between the "old" and the newly formed IPECs. The presence of aggregates at different stages of the equilibration process after a short mixing time could also explain the decreasing polydispersity of the IPECs during the 10 days of mixing.

The same aggregates at $Z = 1$ after 1 h mixing time were also analyzed by scanning force microscopy (SFM) on polished silicon wafers. Figure 4C provides an overview (2.0 × 2.0 μm, height image, *z*-scale = 7 nm) with several IPECs of similar size and shape, and Figure 3D shows the height image of two single IPECs. The single

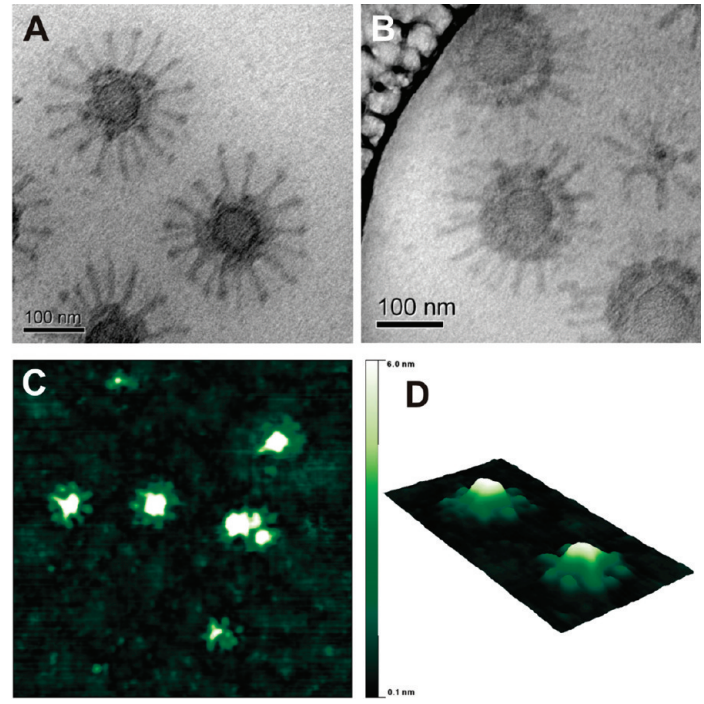


**Figure 4. (A,B) Cryo-TEM micrograph of IPECs at $Z(\pm) = 1$ and pH 10 after 1 h mixing time at different locations of the same sample; (C,D) SFM height images of an IPEC solution at $Z(\pm) = 1$ and pH 10 after deposition on a carbon-coated TEM grid (image size is 2 × 2 μm (C) and 1 × 0.5 μm (D); *z*-scale in both cases is 6 nm), with D displaying an enlargement of C.**

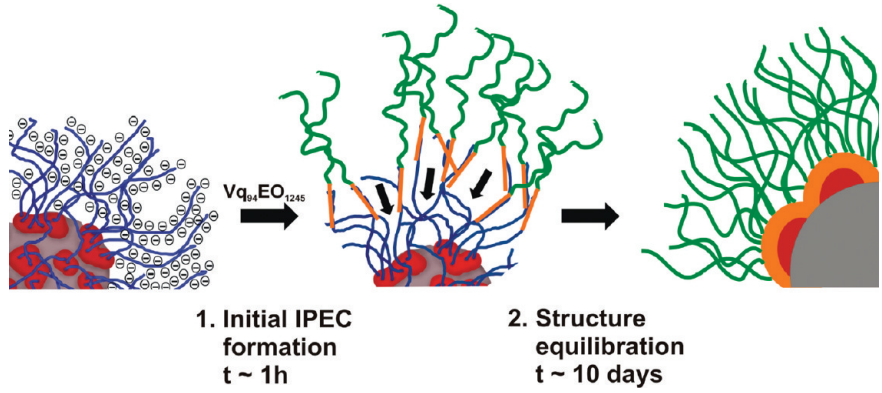


**Figure 5. Schematic depiction of the formation of the star-like intermediate structures of the IPECs between $B_{800}Vq_{190}MAA_{550}$ and $Vq_{94}EO_{1245}$; please note that the precursor micelles on the left are shown according to an "on-top" view, whereas the IPEC on the right is shown as a cross section.**

IPECs in Figure 4D have an overall radius of around 150 nm with a core of 75 nm and nine bumps of 10−15 nm surrounding both. The increase in size is caused by the flattening of the aggregates on the silicon substrate. Also the arms seem to be less stretched than in the corresponding cryo-TEM micrographs (Figure 4A,B).

The (according to DLS) equilibrated IPECs at $Z(\pm) = 1$ after 10 days mixing were also analyzed by cryo-TEM. The resulting cryo-TEM micrographs are shown in Figure 6.

Indeed, the appearance of the structures has significantly changed. Instead of the former core-patchy shell−corona micelles, now a thick, fuzzy, continuous shell can be observed. The core size has remained constant; in both cases, a radius of 30−35 nm was measured. The shell thickness is around 20−30 nm. We propose that this continuous shell is made of both the former, intramicellar IPEC and the newly formed one between excess PMAA and $Vq_{94}EO_{1245}$. As expected, the two different parts of the IPEC shell are not distinguishable. The rather fuzzy appearance of the micellar shell could be due to an incomplete mixing of the two IPEC shells. According to the volume of the newly formed IPEC shell compared to the volume of the two polyelectrolyte chains participating (243 PMAA chains[13] with a DP of 360 and ~900 P2VPq chains with a DP of 94), it is quite likely that also PEO chains are incorporated or buried into this shell. This would also lead to a certain swelling of this shell through the solvent, water. A PEO corona, surrounding the shell, is expected, though not visible in cryo-TEM. However, charge neutrality of the outmost part of the micellar aggregates can be assumed as the micelles do not show repulsion apparent through a strongly deviating core-to-core distance. To confirm this, the zeta-potential of these solutions was determined, revealing −35.8 mV ($B_{800}Vq_{190}MAA_{550}$ precursor micelles), + 14.7 mV ($Vq_{94}EO_{1250}$ diblock copolymer in aqueous solution), and + 0.2 mV (resulting IPEC at $Z = 1$) at comparable concentrations ($c \approx 1$ g/L). Although one has to be careful about a quantitative

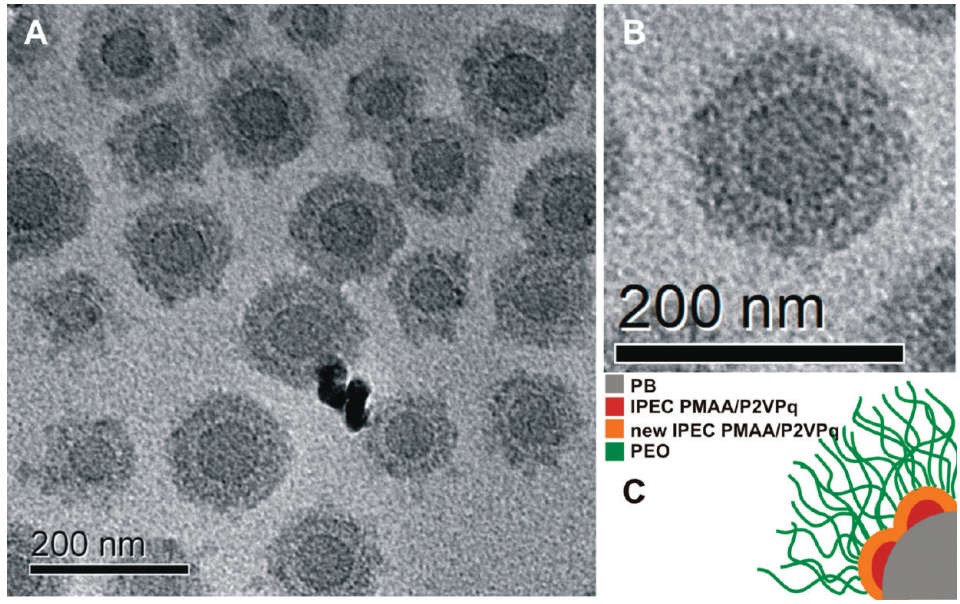


**Figure 6. Cryo-TEM micrograph of the IPEC formed between $B_{800}Vq_{190}MAA_{550}$ and $Vq_{94}EO_{1245}$ at $Z(\pm) = 1$ after 10 days mixing time (A); enlargement of a single IPEC (B); proposed structure of the assembly (C).**

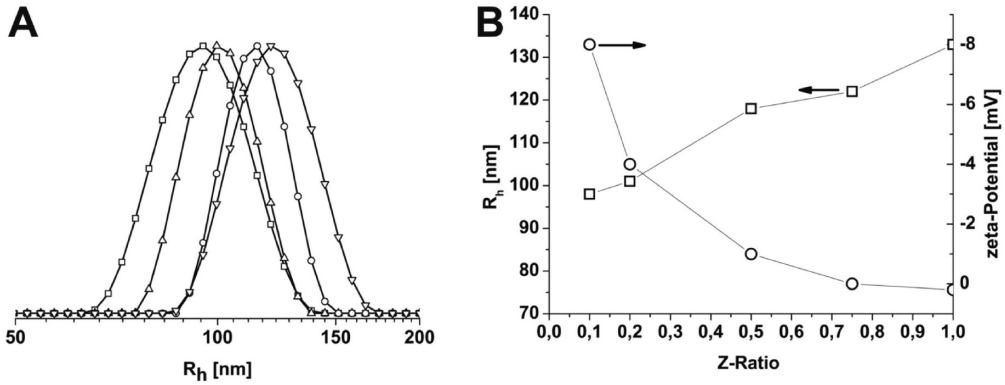


**Figure 7. DLS CONTIN plots for IPECs of $B_{800}Vq_{190}MAA_{550}$ and $Vq_{94}EO_{1245}$ after 10 days mixing at different $Z(\pm) = 0.1$ ($<R_h>_z = 98$ nm, PDI = 1.17, □), 0.2 ($<R_h>_z = 102$ nm, PDI = 1.16, △), 0.5 ($<R_h>_z = 117$ nm, PDI = 1.11, ○), and 0.75 ($<R_h>_z = 123$ nm, PDI = 1.12, ▽) (A); hydrodynamic radii (□) and zeta-potential (○) depending on the prepared $Z(\pm)$ ratio (B).**

evaluation of these measurements, the general message is quite clear. At $Z = 1$, almost uncharged particles are obtained.

**Effect of the Overall $Z(\pm)$ Ratio.** All data presented so far have been obtained for $Z(\pm) = 1$. To elucidate the effect of this ratio on particle size, micelle polydispersity, or the remaining particle charge, we prepared IPECs at different $Z$ values of 0.1, 0.2, 0.5, and 0.75. DLS CONTIN plots and zeta-potential measurements for these solutions after 10 days mixing are shown in Figure 7.

With increasing $Z$, the radius of the IPECs measured by DLS increases steadily. In the beginning, for $Z = 0.1$ and $<R_h>_z = 98$ nm (PDI = 1.17), almost no change can be seen as compared to the block terpolymer precursor micelles ($<R_h>_z = 99$ nm, PDI = 1.18). At $Z = 0.2$, the radius increases slightly to 102 and the distribution narrows (PDI = 1.16). This effect becomes more pronounced at higher $Z$ values ($Z = 0.5$, $<R_h>_z = 117$ nm, PDI = 1.11; $Z = 0.75$, $<R_h>_z = 123$ nm, PDI = 1.12; $Z = 1.0$, $<R_h>_z = 133$ nm, PDI = 1.08). The measured zeta-potential for these solutions follows the same trend: −8 mV ($Z = 0.1$), −6 mV ($Z = 0.2$), −2.5 mV ($Z = 0.5$), −0.2 mV ($Z = 0.75$), and +0.2 mV ($Z = 1.0$) were obtained. The zeta-potential at $Z = 0.75$ does not seem to be different from that for $Z = 1$. We assume that, in this case, the shell of the $B_{800}Vq_{190}MAA_{550}$ precursor micelles is already completely covered with $Vq_{94}EO_{1245}$ molecules, burying any remaining uncomplexed PMAA within the IPEC shell.

To further increase the complexity of these dynamic multicompartmental systems, the preparation of gold nanoparticles inside the IPECs was tested. We therefore prepared IPEC solutions at $Z(\pm) = 0.2$.

**Nanoparticle Generation inside the IPECs.** There is a general and growing interest in the generation of gold nanoparticles within or on polymeric scaffolds,[20,30] for applications in either electronic or catalytic devices. There are several examples about the ability of PAA, PMAA, or comparable weak polyelectrolytes as carriers for noble metal nanoparticles in the literature. For example, Bi *et al.* generated Ag nanoparticles inside the PAA core of PS-*b*-PAA diblock copolymer micelles in toluene.[31] Caruso *et al.* reported the loading of PbS and Au nanoparticles on polymer spheres coated with PAA/poly(allylamine hydrochloride) (PAH) multilayers.[32] To elucidate the use of the presented IPECs as carriers for gold nanoparticles, they were mixed with $HAuCl_4$ in solution. The precursor micelles with a PMAA corona serve as a reference system. For the system presented here, both PMAA and P2VPq could serve as stabilizers for Au NPs. However, we assume that the P2VPq compartments are almost completely located within the collapsed IPEC domains and, hence, by far less accessible for the $AuCl_4^-$ ions. Even so, it cannot be completely neglected that some metal particles are located at either the P2VPq or the IPEC. Typically, the PMAA chains of both the reference system and the IPEC at $Z = 0.2$ were loaded with 10% $HAuCl_4$, calculated on the proposed remaining DP for PMAA of 360[13] in combination with the charge ratio. After 24 h in the dark and subsequent

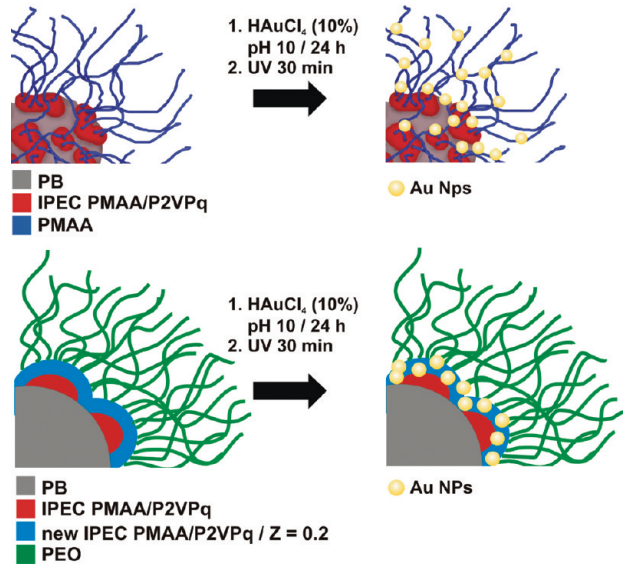


**Figure 8. Schematic depiction of the formation of Au nanoparticles on negatively charged $B_{800}Vq_{190}MAA_{550}$ terpolymer micelles (upper scheme), and IPECs from $B_{800}Vq_{190}MAA_{550}$ and $Vq_{94}EO_{1245}$ at $Z(\pm) = 0.2$ after mixing for 10 days (lower scheme).**

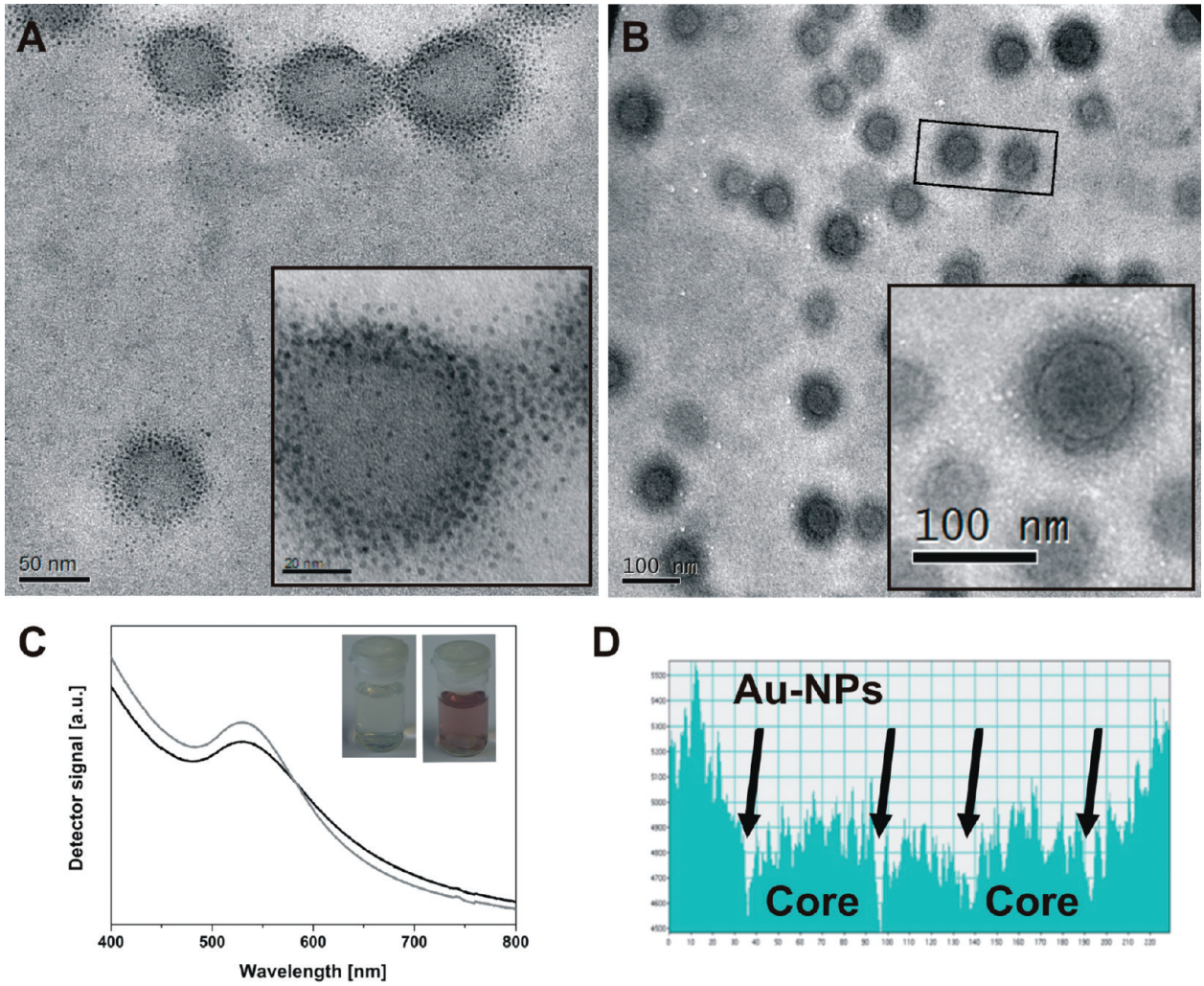


**Figure 9. (A) TEM micrograph of $B_{800}Vq_{190}MAA_{550}$ terpolymer micelles loaded with Au NPs on a carbon-coated copper grid; the inset displays an enlargement. (B) Cryo-TEM micrograph of the IPEC at $Z = 0.2$ loaded with Au NPs; the inset shows an enlargement. (C) UV−vis spectra of both the $B_{800}Vq_{190}MAA_{550}$ micelles (solid black line) and the IPEC (solid gray line) loaded with Au NPs; the insets are photographs taken of the IPEC solutions before (left) and after (right) nanoparticle formation. (D) Gray scale analysis of two adjacent IPECs in B (marked *via* the black rectangle), highlighting the location of the nanoparticles inside the structure.**

dialysis for another 24 h to remove noncoordinated $HAuCl_4$, the solutions were exposed to UV irradiation for 30 min. Afterward, pink solutions were obtained. The reaction scheme is shown in Figure 8.

For the IPECs prepared at $Z = 0.2$, the newly formed shell still exhibits a negative charge and, hence, uncomplexed PMAA units, thus enabling the formation of gold nanoparticles within the IPEC. This was confirmed by zeta-potential measurements (*cf.* Figure 7B). According to the proposed solution structure of the IPECs, the Au NPs should be formed within the shell shielded from the outside by the PEO corona. Here we assume that, for this charge ratio, the equilibrium structure is comparable but with uncomplexed PMAA present. After loading with the Au NPs, the $B_{800}V_{190}MAA_{550}$ terpolymer micelles were analyzed by TEM. The nanoparticle loading of the IPECs was investigated by cryo-TEM. The results are shown in Figure 9.

As depicted in Figure 9A, the Au nanoparticles formed within the PMAA shell of the $B_{800}Vq_{190}MAA_{550}$ micelles are narrowly distributed and around 3−4 nm in diameter, as shown in the enlargement in Figure 9A. They are densely located directly within the IPEC shell around the soft PB core and less packed with growing distance. The patchy shell of these micelles is not visible here as the contrast of the metal particles simply is too high compared to the different block polymer compartments. Strikingly, only very few free Au NPs can be seen, indicating a strong tendency of the $HAuCl_4$ precursor to coordinate within the IPEC shell or the PMAA corona. Figure 5B shows a cryo-TEM of the IPEC solution at $Z = 0.2$ after being loaded with Au NPs in a similar manner. Round-shaped objects with a radius of 60−75 nm can be seen, each exhibiting a thin dark ring inside the gray shell. These must be the Au NPs, located within the IPEC shell and still surrounded by the PEO corona. This is highlighted more clearly in the inset in Figure 8B showing an enlargement of one single IPEC. A thin, continuous dark ring with a thickness of around 5 nm is embedded within the gray IPEC micelle. Furthermore, al-

most no free nanoparticles can be observed in the cryo-TEM in Figure 9B.

Besides electron microscopy, UV−vis spectroscopy is one of the standard methods to determine the aggregation state of noble metal colloids in solution.[33] UV−vis spectra of the $B_{800}Vq_{190}MAA_{550}$ micelles (solid black line) and the IPECs loaded with Au NPs (solid gray line) are shown in Figure 9C. In both cases, an absorption maximum at around 520 nm was obtained, also indicating the formation of rather small gold particles without further aggregation occurring. The inset is two photographs taken from the IPEC solution before (left) and after (right) Au NP formation. The pink color in the right image supports the drawn conclusions. In addition, gray scale analysis on two adjacent IPECs was performed and is depicted in Figure 9D. The sharp insections (arrows) on both sides of the cores present the thin dark ring and, thus, the nanoparticles. Both electron microscopic and spectroscopic techniques convincingly show that the formation of Au NPs selectively within the IPEC shell of complex particles in solution was successfully performed.

## CONCLUSION

We have successfully prepared dynamic and multicompartmental colloidal objects with a radius of around 100−150 nm through the combination of three inherently different approaches: nonsolvent induced self-assembly, ionic complexation, and coordination chemistry. IPEC formation between negatively charged core-patchy shell−corona micelles from $B_{800}Vq_{190}MAA_{550}$ terpolymers and positively charged $Vq_{94}EO_{1250}$ diblock copolymers rendered core−shell−shell−corona objects, which showed a dynamic relaxation behavior within 10 days, changing from a star-like to a spherical shape. The remaining charge of these colloids could be adjusted *via* the mixing ratio of both polymers. The IPECs could be even further modified through the *in situ* reduction of $HAuCl_4$ through UV irradiation within the IPEC shell, resulting in narrowly distributed Au NPs with a diameter of 3−4 nm. These systems could be interesting candidates for catalytic application or act as carriers for sensitive substances through the protective PEO corona.

## METHODS

**Synthesis.** The synthesis and characterization of poly(2-vinyl pyridine)-*block*-poly(ethylene oxide)[18] and polybutadiene-*block*-poly(2-vinyl pyridine)-*block*-poly(*tert*-butylmethacrylate)[34] as well as its modification into polybutadiene-*block*-poly(1-methyl-2-vinylpyridinium)-*b*-poly(methacrylic acid)[13] have been described elsewhere.

**Quaternization.** Poly(2-vinyl pyridine)-*b*-poly(ethylene oxide) $V_{94}EO_{1245}$ (1 g, 0.015 mmol) was dissolved in dioxane (50 mL). A 20-fold excess of dimethyl sulfate (3.56 g, 28 mmol, calculated with a degree of polymerization of 94 for the P2VP) was added *via* syringe. After stirring at 40 °C for 5 days, the excess of dimethyl sulfate was removed by dialysis (regenerated cellulose membranes, MWCO 3.500 g/mol, spectra/por) against deionized water. Poly(*N*-methyl-2-vinylpyridinium)-*b*-poly(ethylene oxide) was obtained *via* freeze-drying. The degree of quaternization was estimated *via* FTIR measurements and was around 80%.[13]

**Preparation of the Interpolyelectrolyte Complexes.** Both $Vq_{94}EO_{1245}$ (5 g/L) and $B_{800}Vq_{190}MAA_{550}$ (1 g/L) were dissolved in a pH 10 buffer solution (VWR, AVS Titrinorm). Afterward, the corresponding volumes to reach a certain *Z* value (overall ratio of positive to negative charges) were mixed in small glass vials and stirred at room temperature.

**Preparation of the Au Nanoparticles.** $HAuCl_4$ was dissolved in deionized water (1 g/L) and kept in the dark. The Au load was calculated according to the number of uncomplexed PMAA units present in solution (depending on the *Z* value in case of the IPECs). Typically, the Au load was 10% or 0.1 equiv compared to the number of PMAA units. The necessary amount of $HAuCl_4$ in solution was added to the micellar solution at pH 10, stirred for 24 h at room temperature, and kept dark. Excess of $HAuCl_4$ was removed afterward *via* dialysis against pH 10 buffer solution (RC membranes, MWCO 3.500 g/mol, spectra/por). Already after this step, the solutions appeared slightly purple, indicating the formation of Au nanoparticles. For the final nanoparticle formation, the solution was exposed to UV irradiation (Hoenle VG UVAHAND 250 GS) for 30 min.

**Dynamic Light Scattering.** DLS measurements were performed in sealed cylindrical scattering cells ($d$ = 10 mm) at an angle of 90° on an ALV DLS/SLS-SP 5022F equipment consisting of an ALV-SP 125 laser goniometer with an ALV 5000/E correlator and a He−Ne laser with the wavelength $\lambda$ = 632.8 nm. The CONTIN algorithm was applied to analyze the obtained correlation functions. Apparent hydrodynamic radii were calculated according to the Stokes−Einstein equation. Prior to the light scattering measurements, the sample solutions were filtered using Millipore Nylon filters with a pore size of 1.2 or 5 μm. Apparent polydispersities for the aggregates in solutions were calculated using the cumulant analysis.

**Transmission Electron Microscopy.** TEM images were taken with a Zeiss CEM902 EFTEM electron microscope operated at 80 kV or a Zeiss EM922 OMEGA EFTEM electron microscope operated at 200 kV. Both machines were equipped with an in-column energy filter. Samples were prepared through deposition of a drop of micellar solution (concentration always 0.1 g/L) onto the TEM grid (gold, 400 mesh). Afterward, the remaining solvent was removed with a blotting paper.

**Cryogenic Transmission Electron Microscopy.** For Cryo-TEM studies, a drop (~2 μL) of the sample solution ($c \approx$ 0.1 wt %) was placed on a lacey carbon-coated copper TEM grid (200 mesh, Science Services, München, Germany), where most of the liquid was removed with blotting paper, leaving a thin film stretched over the grid holes. The specimens were shock vitrified by rapid immersion into liquid ethane in a temperature-controlled freezing unit (Zeiss Cryobox, Zeiss NTS GmbH, Oberkochen, Germany) and cooled to approximately 90 K. The temperature was monitored and kept constant in the chamber during all of the preparation steps. After freezing the specimens, they were inserted into a cryo-transfer holder (CT3500, Gatan, München, Germany) and transferred to a Zeiss EM922 OMEGA EFTEM instrument. Examinations were carried out at temperatures around 90 K. The transmission electron microscope was operated at an acceleration voltage of 200 kV. Zero-loss filtered images ($\Delta E$ = 0 eV) were taken under reduced dose conditions. All images were registered digitally by a bottom-mounted CCD camera system (Ultrascan 1000, Gatan), combined, and processed with a digital imaging processing system (Gatan Digital Micrograph 3.9 for GMS 1.4).

**Scanning Force Microscopy.** SFM images were recorded on a Digital Instruments Dimension 3100 microscope operating in tapping mode. Samples were prepared on polished silicon wafers through dip-coating. The wafer was previously cleaned in toluene, dried on a heating plate, and finally treated with a snow jet. Afterward, the precleaned silicon wafers were dipped into the

sample solution for 20 s, and the excess of solution was afterward removed with a dust-free blotting paper. All images were treated with the Nanoscope 7.20 software.

**Zeta-Potential.** The zeta-potential was determined on a Malvern Zetasizer Nano ZS in conjunction with an MPT2 autotitrator (Malvern). The electrophoretic mobilities ($u$) were converted into $\zeta$ potentials *via* the Smoluchowski equation, $\zeta = u\eta/\varepsilon_0\varepsilon$, where $\eta$ denotes the viscosity and $\varepsilon_0\varepsilon$ the permittivity of the solution.

**UV—Vis Spectroscopy.** The UV spectra of the gold nanoparticle solution were recorded on a Hitachi U-3000 spectrophotometer with a scanning speed of 300 nm/min and a sampling interval of 0.50 nm.

*Acknowledgment.* We thank Jiayin Yuan for performing the UV−vis measurements, Markus Hund for help during the SFM measurements, and Katharina Schatz for help with the illustrations. The Volkswagenstiftung is gratefully acknowledged for financial support within the framework "Complex Materials".

## REFERENCES AND NOTES

1. Lazzari, M.; Lopez-Quintela, M. A. Block Copolymers as a Tool for Nanomaterial Fabrication. *Adv. Mater.* **2003**, *15*, 1583.
2. Ruzette, A.; Leibler, L. *Nat. Mater.* **2005**, *4*, 19.
3. Walther, A.; Andre, X.; Drechsler, M.; Abetz, V.; Müller, A. H. E. Janus Discs. *J. Am. Chem. Soc.* **2007**, *129*, 6187–6198.
4. Bates, F. S.; Fredrickson, G. H. Block Copolymers—Designer Soft Materials. *Phys. Today* **1999**, *52*, 32–38.
5. Goldacker, T.; Abetz, V.; Stadler, R.; Erukhimovich, I.; Leibler, L. Non-centrosymmetric Superlattices in Block Copolymer Blends. *Nature* **1999**, *398*, 137–139.
6. Ludwigs, S.; Böker, A.; Voronov, A.; Rehse, N.; Magerle, R.; Krausch, G. Self-Assembly of Functional Nanostructures from ABC Triblock Copolymers. *Nat. Mater.* **2003**, *2*, 744–747.
7. Guo, S.; Rzayev, J.; Bailey, T. S.; Zalusky, A. S.; Olayo-Valles, R.; Hillmyer, M. A. Nanopore and Nanobushing Arrays from ABC Triblock Thin Films Containing Two Etchable Blocks. *Chem. Mater.* **2006**, *18*, 1719–1721.
8. Erhardt, R.; Zhang, M.; Böker, A.; Zettl, H.; Abetz, C.; Frederik, P.; Krausch, G.; Abetz, V.; Müller, A. H. E. Amphiphilic Janus Micelles with Polystyrene and Poly(methacrylic acid) Hemispheres. *J. Am. Chem. Soc.* **2003**, *125*, 3260–3267.
9. Li, Z.; Hillmyer, M. A.; Lodge, T. P. Morphologies of Multicompartment Micelles formed by ABC Miktoarm Star Terpolymers. *Langmuir* **2006**, *22*, 9409–9417.
10. Cui, H.; Chen, Z.; Zhong, S.; Wooley, K. L.; Pochan, D. J. Block Copolymer Assembly *via* Kinetic Control. *Science* **2007**, *317*, 647–650.
11. Kabanov, V. A. Polyelectrolyte Complexes in Solution and in Bulk. *Russ. Chem. Rev.* **2005**, *74*, 3–20.
12. Pergushov, D. V.; Remizova, E. V.; Feldthusen, J.; Zezin, A. B.; Müller, A. H. E.; Kabanov, V. A. Novel Water Soluble Micellar Interpolyelectrolyte Complexes. *J. Phys. Chem. B* **2003**, *107*, 8093–8096.
13. Schacher, F.; Walther, A.; Müller, A. H. E. Dynamic Multicompartment-Core Micelles in Aqueous Media. *Langmuir* **2009**, DOI: 10.1021/la901182c.
14. Burkhardt, M.; Martinez-Castro, N.; Tea, S.; Drechsler, M.; Babin, I. A.; Grishagin, I. V.; Schweins, R.; Pergushov, D. V.; Gradzielski, M.; Zezin, A. B.; Müller, A. H. E. Polyisobutylene-*block*-Poly(methacrylic acid) Diblock Copolymers: Self-Assembly in Aqueous Media. *Langmuir* **2007**, *23*, 12864–12874.
15. Burkhardt, M.; Ruppel, M.; Tea, S.; Drechsler, M.; Schweins, R.; Pergushov, D. V.; Gradzielski, M.; Zezin, A. B.; Müller, A. H. E. Water-Soluble Interpolyelectrolyte Complexes of Polyisobutylene-*block*-Poly(methacrylic acid) Micelles: Formation and Properties. *Langmuir* **2008**, *24*, 1769–1777.
16. Chelushkin, P. S.; Lysenko, E. A.; Bronich, T. K.; Eisenberg, A.; Kabanov, V. A.; Kabanov, A. V. Polyion Complex Nanomaterials from Block Polyelectrolyte Micelles and Linear Polyelectrolytes of Opposite Charge: 1. Solution Behavior. *J. Phys. Chem. B* **2007**, *111*, 8419–8425.
17. Chelushkin, P. S.; Lysenko, E. A.; Bronich, T. K.; Eisenberg, A.; Kabanov, V. A.; Kabanov, A. V. Polyion Complex Nanomaterials from Block Polyelectrolyte Micelles and Linear Polyelectrolytes of Opposite Charge. 2. Dynamic Properties. *J. Phys. Chem. B* **2008**, *112*, 7732–7738.
18. Voets, I. K.; de Keizer, A.; de Waard, P.; Frederik, P. M.; Bomans, P. H. H.; Schmalz, H.; Walther, A.; King, S.; Leermakers, F. A. M.; Cohen Stuart, M. A. Double-Faced Micelles from Water-Soluble Polymers 13. *Angew. Chem., Int. Ed.* **2006**, *118*, 6825–6828.
19. Förster, S.; Antonietti, M. Amphiphilic Block Copolymers in Structure-Controlled Nanomaterial Hybrids. *Adv. Mater.* **1998**, *10*, 195–217.
20. Haryono, A.; Binder, W. H. Controlled Arrangement of Nanoparticle Arrays in Block-Copolymer Domains. *Small* **2006**, *2*, 600–611.
21. He, J.; Tangirala, R.; Emrick, T.; Russell, T. P.; Böker, A.; Li, X.; Wang, J. Self-Assembly of Nanoparticle−Copolymer Mixtures: A Kinetic Point of View. *Adv. Mater.* **2007**, *19*, 381–385.
22. Lin, Y.; Böker, A.; He, J.; Sill, K.; Xiang, H.; Abetz, C.; Li, X.; Wang, J.; Emrick, T.; Long, S.; Wang, Q.; Balazs, A.; Russell, T. P. Self-Directed Self-Assembly of Nanoparticle/Copolymer Mixtures. *Nature* **2005**, *434*, 55–59.
23. Seregina, M. V.; Bronstein, L. M.; Platonova, O. A.; Chernyshov, D. M.; Valetsky, P. M.; Hartmann, J.; Wenz, E.; Antonietti, M. Preparation of Noble-Metal Colloids in Block Copolymer Micelles and Their Catalytic Properties in Hydrogenation. *Chem. Mater.* **1997**, *9*, 923–931.
24. Schmid, G. Large Clusters and Colloids. Metals in the Embryonic State. *Chem. Rev.* **1992**, *92*, 1709–1727.
25. Zheng, P.; Jiang, X.; Zhang, X.; Zhang, W.; Shi, L. Formation of Gold@Polymer Core−Shell Particles and Gold Particle Clusters on a Template of Thermoresponsive and pH-Responsive Coordination Triblock Copolymer. *Langmuir* **2006**, *22*, 9393–9396.
26. Carrot, C.; Valmalette, J. C.; Plummer, C. J. G.; Scholz, S. M.; Dutta, J.; Hofmann, H.; Hilborn, J. G. Gold Nanoparticle Synthesis in Graft Copolymer Micelles. *Colloid Polym. Sci.* **1998**, *276*, 853–859.
27. Valden, M.; Lai, X.; Goodman, D. W. Onset of Catalytic Activity of Gold Clusters on Titania with the Appearance of Nonmetallic Properties. *Science* **1998**, *281*, 1647–1650.
28. Chiu, J. J.; Kim, B. J.; Kramer, E. J.; Pine, D. J. Control of Nanoparticle Location in Block Copolymers. *J. Am. Chem. Soc.* **2005**, *127*, 5036–5037.
29. Lu, J. Q.; Yi, S. S. Uniformly Sized Gold Nanoparticles Derived from PS-*b*-P2VP Block Copolymer Templates for the Controllable Synthesis of Si Nanowires. *Langmuir* **2006**, *22*, 3951–3954.
30. Djalali, R.; Li, S. Y.; Schmidt, M. Amphipolar Core−Shell Cylindrical Brushes as Templates for the Formation of Gold Clusters and Nanowires. *Macromolecules* **2002**, *35*, 4282–4288.
31. Lei, Z.; Wei, X.; Zhang, L.; Bi, S. Amphiphilic Core−Shell Particles as Carrier Systems for Metallic Nanoparticles. *Colloids Surf., A* **2008**, *317*, 705–710.
32. Schuetz, P.; Caruso, F. Semiconductor and Metal Nanoparticle Formation on Polymer Spheres Coated with Weak Polyelectrolyte Multilayers. *Chem. Mater.* **2004**, *16*, 3066–3073.
33. Johnson, P. B.; Christy, R. W. Optical Constants of the Noble Metals. *Phys. Rev. B* **1972**, *6*, 4370–4379.
34. Schacher, F.; Walther, A.; Ruppel, M.; Drechsler, M.; Müller, A. H. E. Multicompartment Core Micelles in Organic Media. *Macromolecules* **2009**, *42*, 3540–3548.